



University of Warwick institutional repository: <http://go.warwick.ac.uk/wrap>

This paper is made available online in accordance with publisher policies. Please scroll down to view the document itself. Please refer to the repository record for this item and our policy information available from the repository home page for further information.

To see the final version of this paper please visit the publisher's website. Access to the published version may require a subscription.

Author(s): D. P. Woodruff

Article Title: The interface structure of n-alkylthiolate self-assembled monolayers on coinage metal surfaces

Year of publication: 2008

Link to published version:

<http://dx.doi.org/10.1039/b813948b>

Publisher statement: None

The interface structure of n-alkylthiolate self-assembled monolayers on coinage metal surfaces

D.P.Woodruff

Physics Department, University of Warwick, Coventry CV4 7AL

Abstract

The current state of understanding of the structure of the metal/thiolate interface of n-alkylthiolate ‘self-assembled monolayers’ (SAMs) on Cu(111), Ag(111) and Au(111) is reviewed. On Cu(111) and Ag(111) there is now clear evidence that adsorbate-induced reconstruction of the outermost metal layer occurs to a less atomically-dense structure, with the S head-group atom bonded to four-fold and three-fold coordinated hollow sites, respectively, and that intermolecular interaction plays some role in the periodicity of the resulting SAMs. On the far more heavily-studied Au(111) surface, the detailed interface structure remains controversial, but there is growing evidence for the role of Au-adatom-thiolate moieties in the layer ordering.

1. Introduction

Normal (unbranched) alkylthiolate, $\text{CH}_3(\text{CH}_2)_{n-1}\text{S}$ -, self-assembled monolayers (SAMs) on coinage metal surfaces (with the number of C atoms, n being in the range from 1 to greater than 20) have been the subject of very many investigations over the last 15 years or more (e.g. [1, 2, 3, 4], with a particular focus on the Au(111) substrate. Such films are commonly formed by the surface reaction of deprotonation of an alkanethiol, but in some cases are also formed by S-S bond scission of a symmetric alkyldisulfide $(\text{CH}_3(\text{CH}_2)_{n-1}\text{S})_2$. More generally, attachment of a wide range of molecular species to such surface through a deprotonated thiol end-group can be exploited for applications as diverse as corrosion protection, chemical and biological sensors, and opto-electronics [5]; they also provide a means of patterning species as varied as DNA (6) and molecular motors (7) to gold surfaces. The fact that evaporated gold films are typically (111) textured, and that most of these species can be deposited from solution, means that they are potentially well-suited to practical applications. However, many of these SAMs can also be prepared under ultra-high vacuum (UHV) conditions on well-characterised single-crystal surfaces, allowing the full armoury of modern surface science methods to be directed to their study. It is investigations based on this UHV methodology that are reviewed here. Note that is common in the literature of these system to describe the SAMs in terms of the specific alkanethiol used in the preparation; here, the notation will be to make the deprotonation explicit by describing the SAMs in terms of the alkylthiolate.

Despite this large number of investigations, there has been surprisingly few quantitative structural studies of the thiolate/metal interface, even for the simplest short-chain, alkylthiolates, and it is this work, and the resulting understanding that is emerging, that is the focus of this short review. More qualitative methods, such as spectroscopic probes (notably infrared spectroscopy of X-ray absorption spectroscopy) have provided valuable information on the conformation and orientation of the alky chains, while scanning probe microscopy (STM) has proved particularly useful in investigating the ordering within the films, even at solid-liquid interfaces. In general, however, these methods do not provide any direct, and certainly no quantitative, information on the S-headgroup/metal interface

structure. As such, they are not reviewed here, but are covered elsewhere [1, 2, 3, 4].

In general, the ordering of a molecular layer on a well-ordered single crystal surface is determined by the balance of two effects. One is the lateral corrugation of the adsorbate-substrate potential which reflects the periodicity of the substrate and the fact that, for an isolated molecule, differently-coordinated sites have different adsorption energies. The other is the role of intermolecular interactions which determine the adsorbate ordering in the absence of the substrate corrugation, with the van der Waals forces between the alkyl chains being thought to be an important factor. ‘Self-assembly’ of a molecular layer tends to imply that it is the intermolecular interactions that dominate the ordering (as in the case of a Langmuir-Blodgett film on a liquid surface). In the case of alkylthiolates on coinage metal surfaces, however, most such layers have long-range ordering that is commensurate with the substrate periodicity, implying that the corrugation of the substrate potential plays a dominant role in the ordering, although intermolecular repulsion must clearly influence the nearest-neighbour spacing within the layers. This may be one reason for the implicit assumption of almost all but the most recent investigations that the molecular layer ordering occurs on an unreconstructed metal surface – i.e. that the substrate simply provides a rigid atomic-scale chequer-board on which the alkylthiolate molecules form their ‘self-assembled’ monolayer structures. Recent detailed structural studies of the thiolate/metal interface on Cu(111), Ag(111) and Au(111) indicate, however, that this is not the case. On the first two of these substrates there is direct and explicit evidence that the outermost metal layer is substantially reconstructed by interaction with the alkylthiolates, leading to a reduced atom density within the layer. On Au(111), the details of the interface structure remain controversial, but here too there is clear evidence of adsorbate-induced reconstruction of the metal surface. In the remainder of this article I will review this evidence for reconstruction and the nature of the thiolate/metal interface for these three substrates.

2. Cu(111)

Copper surfaces are the least-studied of the noble metals for alkylthiolate SAMs, presumably because copper is generally the most reactive of the three metals and thus least well-suited to methods of solution deposition, although some solution deposition results do exist; under suitable conditions the surface oxide may be removed at the solid-liquid interface, allowing reaction with a thiol. Nevertheless, the detailed investigations of a small number of model thiolate/Cu systems does indicate a clear pattern of behaviour. Moreover, the first clear evidence of thiolate-induced reconstruction on coinage metal surfaces was obtained some 20 years ago for the Cu(111)/CH₃S surface phase, formed by UHV reaction with either dimethyldisulfide or methanethiol [8]. This investigation used a combination of SEXAFS (surface extended X-ray absorption fine structure [9, 10]) to determine the S-Cu nearest-neighbour bondlength and bond angle, and NISXW (normal incidence X-ray standing waves [11, 12]) to determine the spacing of the S atoms above the nearest extended-bulk Cu lattice plane. The S-Cu bondlength obtained in this way (2.38 Å) means that, for adsorption on an unreconstructed Cu(111) surface, the S-Cu interlayer spacing must lie within the range from 2.38 Å (atop site) to 1.87 Å (three-fold coordinated hollow site) with an angle of the S-Cu bond relative to the surface normal lying between 0° and 38°. However, the NIXSW measurements gave a layer spacing of 1.20 Å while the S-Cu bond angle given by the SEXAFS results of 60° is consistent with this small value of the layer spacing. Clearly, these values imply that the S headgroup atom must penetrate the outermost Cu atom layer, an arrangement that is only possible if this outermost metal layer has a significant reduction in the atomic density relative to that of the bulk-like close-packed layer of the clean surface.

Initially, it was assumed that this reconstructed layer would have the same hexagonal symmetry as the substrate [13], but identification of the true nature of this reconstructed Cu layer came some years later from an investigation using STM, supported by observation of an associated low energy electron diffraction (LEED) pattern. These results showed that the local arrangement of the thiolate species is on a near-square mesh with dimensions of approximately 4.06 Å x 4.18 Å and an included angle of 88.7° [14],

leading to the proposal of the pseudo-(100) surface reconstruction shown in fig. 1. In this model the outermost Cu atomic layer has a structure similar to that of a Cu(100) surface, albeit with a slightly enlarged Cu-Cu later spacing ($2.88 \text{ \AA} \times 2.95 \text{ \AA}$ compared with $2.55 \text{ \AA} \times 2.55 \text{ \AA}$ on Cu(100)), and the thiolate species occupy alternate four-fold coordinated hollow sites in a $c(2 \times 2)$ mesh relative to that of the reconstructed Cu layer. This layer has only 66% of the atomic density of a close-packed Cu(111) layer. This structure is fully compatible with both the SEXAFS and NIXSW results, as well as the later STM images. Further evidence for this model came from MEIS (medium energy ion scattering [15, 16]) measurements which were shown to be consistent with this number of laterally-displaced Cu atoms in the reconstruction [17]. NIXSW [18] and STM [19] measurements of octylthiolate ($n=8$) on Cu(111) show essentially identical results, indicating that this thiolate-induced reconstruction is not unique to the methyl species, but is evidently more general.

A clear implication of this thiolate-induced reconstruction is that on copper surfaces a fourfold-coordination site of the S headgroup, as provided on this more openly-packed surface, is energetically favoured over a three-fold (or lower) coordinated site on the close-packed Cu(111) surface. In fact this type of adsorbate-induced pseudo-(100) reconstruction of fcc (111) (and (110)) surfaces is not unique to the thiolates, and has been observed for a number of atomic adsorbates (including N on Cu(111), e.g. [20]), although this behaviour is certainly not common for molecular adsorbates. The general rationale for this behaviour is that it occurs if the (100) hollow site adsorption is sufficiently-strongly favoured over adsorption on an unreconstructed surface to overcome the excess energy associated with the interface between the substrate and the reconstructed metal layer [21]. Unfortunately, these pseudo-(100) reconstructions are either incommensurate or have a large commensurate surface mesh (for the thiolates on Cu(111) there is some evidence for a commensurate mesh, denoted in the matrix notation as $\begin{bmatrix} 4 & 3 \\ -1 & 3 \end{bmatrix}$ [14, 17]), so a calculation of the detailed energetics using density functional theory (DFT) is computationally rather challenging.

One unusual feature of the thiolate-induced reconstruction of Cu(111) is that the Cu-Cu spacing within the reconstructed layer is significantly (~15%) larger than on Cu(100), whereas in most other examples of pseudo-(100) reconstructions the spacing is much closer to that of the (100) surface. In this regard, some investigations of thiolates on the Cu(100) surface are relevant. Quantitative determinations of the local adsorption site of the S headgroup atom have been performed for methylthiolate [22] and 2-mercaptobenzoxazole (MBO, C₇H₅NOS) [23] by NIXSW, for hexylthiolate (*n*=6) by SEXAFS [24], and for benzenethiolate (C₆H₅S) by a combination of NIXSW and photoelectron diffraction [25]. In all cases, the adsorption site is the four-fold coordinated hollow site, reinforcing the implication of the Cu(111) studies that this is, indeed, an energetically-favoured site. However, an interesting feature of the long-range ordering of these adsorbates on Cu(100) is that none of these systems show a c(2x2) 0.5 ML structure at saturation coverage that would correspond to an inter-adsorbate spacing of 3.61 Å. Instead, all show an ordered (2x2) (0.25 ML) ordered phase (inter-adsorbate spacing 5.11 Å), while at higher coverage the methyl-, hexyl- and benzenethiolate species all show a c(2x6) ordering. STM images of both the alkylthiolate species do show *local* c(2x2) ordering within the c(2x6) phase, but this phase either involves top-layer rumpling [22] or missing rows [24] of thiolate species. By contrast, relative to the pseudo-(100) surface on Cu(111), the thiolate structures *are* c(2x2). The implication is that the intermolecular repulsion is too strong at the separation of 3.61 Å, thus providing a rationale for the larger periodicity of the pseudo-(100) reconstructed layer on Cu(111), in which the shortest intermolecular distance is 4.06 Å. We might infer, therefore, that the alkylthiolate layers on Cu(111) really are '*self*'-assembled, in that the intermolecular spacing is determined (or at least strongly influenced) by intermolecular interactions, while it is the thiolate that drives the reconstruction of the copper surface. We should note, though, that atomic S also forms a (2x2), but not a c(2x2), overlayer on Cu(100) [26], so this inferred inter-adsorbate short-range repulsion at a spacing of 3.61 Å is not necessarily a result of the alkyl chain. Coincidentally, atomic S also causes a reconstruction of Cu(111) surfaces (e.g.[27]), generally not to a pseudo-(100) structure, although there is some evidence of such a phase [28].

3. Ag(111)

On Ag(111) there is also clear evidence of thiolate-induced reconstruction, although the detailed behaviour differs significantly from that of Cu(111). An early spectroscopic investigation of methylthiolate on Ag(111) showed that it yields a LEED pattern corresponding to $(\sqrt{7}\times\sqrt{7})R19.1^\circ$ ordering [29]. The fact that atomic S was known to give an ordered phase on this surface (but that the spectroscopic data showed clearly that the thiolate was *not* dissociated in this study) with the same periodicity led to an assumption that the two structures have strong similarities. In the case of the atomic S phase, the structure has been attributed to multilayers of f-cubic $\text{Ag}_2\text{S}(111)$ which has a very close match in lattice parameter [30]. One feature of this bulk sulphide structure is that within the $(\sqrt{7}\times\sqrt{7})$ unit mesh are three equally-spaced S atoms, thus defining a sub-mesh with a periodicity of $\sqrt{7/3}$ times that of the Ag(111) substrate (i.e. 4.41 Å), and the thiolate S headgroup atoms on Ag(111) have been assumed to occupy this same lateral sub-mesh. An implicit assumption seems to have been made that these thiolate species are adsorbed onto an unreconstructed Ag(111) substrate, although this model implies three different adsorption sites for the three thiolate species per $(\sqrt{7}\times\sqrt{7})$ unit mesh.

Initial STM studies of the methylthiolate adsorption phase showed, under different tip conditions, either the $\sqrt{7}$ periodicity of the true commensurate surface mesh or the $\sqrt{7/3}$ periodicity implied for the thiolate sub-mesh [31], while more recently we have reported images that show both periodicities simultaneously [32]; all observed atomic protrusions are on a $\sqrt{7/3}$ mesh, but one third of these, on a regular $\sqrt{7}$ mesh, are slightly higher above the surface than the others. These observations seem to confirm the idea that the thiolate species do lie on the expected submesh, but still provide no detailed information on the interface structure. More quantitative information comes from NIXSW measurements [33] which, as in the case of Cu(111), yield S-Ag interlayer spacings too small to be consistent with any combination of pure overlayer sites. In this case too, the implication is that there must be a reconstructed, lower-density, outermost Ag layer providing enlarged hollow sites for thiolate adsorption at a lower height above the surface. A number of possible models of the reconstruction have been considered in

interpreting the results of the NIXSW experiments, and also of a MEIS investigation of the number of laterally-displaced Ag atoms [34]. Notice that the hexagonal symmetry of the $(\sqrt{7}\times\sqrt{7})$ unit mesh clearly implies that the reconstruction must retain this symmetry and thus cannot, as in the case of Cu(111), involve a pseudo-(100) reconstruction. The model which gives the best fit to these experimental data is shown in fig. 2 and comprises a reconstructed Ag layer with an atomic density of $3/7$ ML, with $3/7$ ML of thiolate species bound by the S headgroup atom to the (enlarged) three-fold coordinated hollow sites in this reconstructed layer. We may note that the local S-Ag coordination and structure in this model is very similar to that in f-cubic $\text{Ag}_2\text{S}(111)$.

More recently Torres *et al.* [35] have reported the results of DFT calculations of the $\text{Ag}(111)$ $(\sqrt{7}\times\sqrt{7})\text{R}19.1^\circ\text{-CH}_3\text{S}$ structure and arrive at a very surprising conclusion: namely, that the total energy of the simple overlayer structure and two slightly different versions of the reconstruction model favoured by the NIXSW and MEIS studies are (within the precision of the calculations) essentially identical. This led them to suggest that the different structures may coexist in different relative amounts depending on the method of preparation. Such a conclusion cannot, of course, be universally refuted without very many further experiments; one really needs to know what preparation conditions would favour each structure. However, what is certainly true is that all the UHV preparations of the phase made in the NIXSW and MEIS experiments are clearly inconsistent with any significant occupation of an unreconstructed phase.

One interesting feature of the $\text{Ag}(111)$ /alkylthiolate system is that while there is universal acceptance that methylthiolate leads to a commensurate $(\sqrt{7}\times\sqrt{7})\text{R}19.1^\circ$ phase, there is conflicting evidence as to whether longer-chain alkylthiolates also lead to the same commensurate phase or to an ordering similar to that of the $(\sqrt{7}\times\sqrt{7})\text{R}19.1^\circ$ phase, but with slightly larger intermolecular separations. Specifically, an investigation of the $n=18$ alkylthiolate on $\text{Ag}(111)$ using X-ray diffraction and low-energy (He) atom diffraction (LEAD) led to the conclusion that, for this species, an ordered phase having two rotational domains similar to that of the $(\sqrt{7}\times\sqrt{7})\text{R}19.1^\circ$ structure is formed, but the lateral periodicity is $\sim 6\%$ larger than this commensurate structure [36]. Subsequently, one STM

study of decanethiolate ($n=10$) on Ag(111) [37] came to a similar conclusion, while most recently our own STM and LEED measurements on the pentylthiolate ($n=5$) layer also indicated an enlarged, incommensurate, surface unit mesh [38]. As a general rule, establishing whether the overlayer is commensurate or incommensurate by measuring nearest-neighbour interatomic distances in STM, or measuring the exact location of diffracted beams corresponding to the surface layer sub-mesh in a conventional diffraction technique (particularly using a standard LEED optics), can place significant demands on the precision of the measurement. However, the presence or absence of the real-space or reciprocal-space features associated with the larger ($\sqrt{7}\times\sqrt{7}$) commensurate ‘super-mesh’ of the substrate and overlayer is a more qualitative characteristic of the commensurate and incommensurate phases, and in the case of the pentylthiolate system, at least, the data show the clear signature in both LEED and STM of incommensuration. An incommensurate ordered structure with a larger lateral periodicity than that of the related commensurate mesh, of course, is a clear indicator of a dominant role of intermolecular interactions, and could be taken to indicate true ‘*self-assembly*’, although in this case it seems that these intermolecular forces are repulsive. In this context, though, it is interesting to note that NIXSW measurements of overlayers of both octylthiolate [39] and pentylthiolate [38] indicate the small S/Ag interlayer spacings found for methylthiolate, indicating that these phases must involve a similar reconstruction of the outermost Ag layer to that seen for the commensurate methylthiolate phase. In some ways this situation is similar to that of the pseudo-(100) reconstruction of Cu(111) by methylthiolate and octylthiolate; in both cases it seems that the lateral periodicity of the reconstructed layer is influenced by intermolecular repulsion. However, on Ag(111) there is clear evidence that there is some dependence of this spacing on the alkyl chain length, whereas on Cu(111), no such evidence has been reported, although no precise comparison of the Cu-Cu distances in for methyl- and octylthiolate was performed.

4. Au(111)

4.1 Overview

The Au(111) surface remains much the most-investigated substrate for alkylthiolate

SAMs, as well as for a range of other more complex thiolate-bonded molecular species. Despite this, the number of experimental investigations seeking to quantify the interface structure remains modest, and there is no clear consensus in the interpretation.

An important general feature of the structural properties of the alkylthiolates on Au(111) is the existence of a number of different long-range ordered structural phases, identified by diffraction methods and by STM. In general, for each chain length, there are three main structural phases with unit meshes of $(m \times \sqrt{3})$ rect., $(\sqrt{3} \times \sqrt{3})R30^\circ$ and $(2\sqrt{3} \times 3)$ rect.[†] (e.g. [2, 3, 72, 40]). The $(m \times \sqrt{3})$ rect. structures correspond to the so-called striped phases in which the molecules ‘lie down’ on the surface and the value of m , which depends on the alkyl chain length, is such as to create a unit mesh approximately 2x the alkyl chain length, implying a coverage of two molecules per surface unit mesh. It is generally assumed that these two molecules have their S head-group atoms at opposite ends within the unit mesh, but are in symmetrically-equivalent geometries (fig. 3). The $(\sqrt{3} \times \sqrt{3})R30^\circ$ and $(2\sqrt{3} \times 3)$ rect. structures are both ‘standing-up’ phases in which the alkyl chain is typically tilted from the surface normal by $\sim 30^\circ$. Other ordered phases have been observed; for example, for some of the longer alkyl chains, phases that appear to correspond to an intermediate tilt angle of the chain of $\sim 50^\circ$ are seen at intermediate coverages to those of the ‘lying-down’ and ‘standing-up’ phases [41]. Here we consider only the three main phases mentioned above.

Both the $(\sqrt{3} \times \sqrt{3})R30^\circ$ and the $(2\sqrt{3} \times 3)$ rect. phases are believed to correspond to a coverage of 0.33 ML, so while in the $(\sqrt{3} \times \sqrt{3})R30^\circ$ this implies one molecule per surface unit mesh, with all the molecules in equivalent sites, the $(2\sqrt{3} \times 3)$ rect. unit mesh is four times larger in area, thus containing four molecules per unit mesh with at least two different local geometries. The STM images of $(2\sqrt{3} \times 3)$ rect. show significant variations, leading to suggestions for dodecylthiolate ($n=12$), for example, that this unit mesh may be associated with as many as five distinctly different structures [42]. However, there is

[†] The $(2\sqrt{3} \times 3)$ rect. phase is referred to in much of the SAM literature as ‘c(4x2)’, though what is meant by this is actually c(4x2) relative to the $(\sqrt{3} \times \sqrt{3})R30^\circ$ mesh, not relative to the (1x1) substrate mesh. We will not make use of this nomenclature which is inconsistent with standard practices of surface crystallography.

evidence that artefacts of the technique associated with tip and imaging conditions are the cause of these differences [43], and that the images all correspond to only one $(2\sqrt{3}\times 3)$ rect. structure. Indeed, characteristic absences of certain diffracted beams in X-ray diffraction studies [44, 45, 46] of the $(2\sqrt{3}\times 3)$ rect. phase indicate that there can only be two distinctly different local adsorption geometries involved. The basis of this conclusion [45] is illustrated in fig. 4 which shows a model of the real-space structure and the related diffraction pattern, with the diffracted beams labelled according to the $(2\sqrt{3}\times 3)$ rect. mesh. The general equation governing the geometrical structure factor for a structure defined within a two-dimensional mesh is:

$$F_{hk} = \sum_{j=1}^N f_j \exp[2\pi i(hx_j + ky_j)]$$

where (h,k) are the diffracted beams, the summation is over all atoms in the unit mesh with coordinates (x,y) , (in units of the unit mesh dimensions), and f_j are the atomic scattering factors. If the f_j are redefined as the scattering factors of the thiolate molecules in a particular orientation, then one can determine any systematic absences (zero values of F_{hk}) by simply summing over the molecules by including only the coordinates of the S headgroup atoms within the overlayer. A key requirement to describe the observed diffraction pattern is that, in the schematic model shown in fig. 3, species 1, which may be defined as at the location $(0,0)$ is identical in orientation to species 1' that is located at the relative position within the unit mesh of $(0.25, 0.50)$. In general, we may put molecule 2 at (x_2, y_2) with a scattering factor f_2 (allowing for a different possible orientation) but require that the species at 2' has the same orientation as that at 2 and that the relative position of 2' is the same as that of 1' to 1, i.e. species 2' is at $(x_2+0.25, y_2+0.50)$. Then:

$$F_{hk} = [f_1 + f_2 \exp 2\pi i(hx_2 + ky_2)][1 + \exp(2\pi i(h/4 + k/2))]$$

The right-hand term of this equation goes to zero when $((h/2)+k)$ is an odd integer – exactly the conditions corresponding to the missing diffracted beams of fig. 3. The implication of this is that there can be only two distinct local geometries of the thiolate species within the $(2\sqrt{3}\times 3)$ rect. unit mesh, and that these are in pairs separated by the relative coordinates $(0.25, 0.50)$. This clearly places significant constraints on the possible structural models of this phase, while semi-quantitative arguments based on the

X-ray diffraction data indicate that the difference between the species at sites 1 and 2 almost certainly involve some inequivalence in S headgroup location and not simply a difference in the orientation of the alkyl chain.

STM studies also show rather clearly that the $(\sqrt{3}\times\sqrt{3})R30^\circ$ and $(2\sqrt{3}\times 3)\text{rect.}$ phases generally coexist in spatially-distinct domains, and that switching between these phases and their relative occupation, by subtle changes in temperature, or perhaps even as a result of sweeping the STM tip over them, occurs rapidly (e.g. [47]). Evidently, these two structural phases must have very similar energies, and switching from one to the other must involve very small energy barriers. Of course, this coexistence also presents a challenge to structure determination by conventional diffraction methods because, as shown in fig. 3, the diffracted beams associated with the $(\sqrt{3}\times\sqrt{3})R30^\circ$ phase are a subset of the diffracted beams associated with the $(2\sqrt{3}\times 3)\text{rect.}$ phase. Measurements of these beam intensities thus reflect some sum of the structure of the two coexistent phases.

These multiple phases raise a number of general, as well as specific, questions about the interface structure. Firstly, what is the (single) local S head-group geometry at the metal interface in the striped and $(\sqrt{3}\times\sqrt{3})R30^\circ$ phases? Secondly, what are the different geometries involved in the $(2\sqrt{3}\times 3)\text{rect.}$ phase; do these involve different S head-group local sites at the interface, or are they associated with changes only in the alignment or ordering of the alkyl chains? In this context, it is notable that there appear to be no reports of the existence of the $(2\sqrt{3}\times 3)\text{rect.}$ phase for methylthiolate (which also has no corresponding striped phase), although a different (3×4) phase of methylthiolate, thought to occur at the same coverage, has been reported to be seen under certain conditions [48, 49]. Finally, why is the transformation between the $(\sqrt{3}\times\sqrt{3})R30^\circ$ and $(2\sqrt{3}\times 3)\text{rect.}$ structures so facile?

The first attempt to apply a truly quantitative experimental technique to determine the interface structure of one of these interfaces seems to have been a SXRD (surface X-ray diffraction) study reported in 1994 of the $(2\sqrt{3}\times 3)\text{rect.}$ phase of decylthiolate ($n=10$) [44]. This led to the rather surprising conclusion that in this structure there is dimerisation of

the adsorbed thiolates to produce a S-S distance of 2.2 Å, rather close to that of a disulphide. In this structure one S headgroup atom is in a three-fold-coordinated hollow site, the other in an off-bridge site. This interpretation has been the subject of considerable debate, but does not appear currently to be widely accepted, although the notion that there may be some ‘pairing’ (in some senses implicit in the discussion of the missing diffracted beams above) remains. One particular objection to the specific model originally proposed is that there is strong evidence [50, 51, 52] that disulphides adsorb by cleavage of the S-S bond to form thiolates, rather than the opposite effect. A later NIXSW investigation of this same system, involving some of the same researchers [53], did favour S-S headgroup pairing, albeit with different local adsorption sites, one S being close to an atop site, with the second (inequivalent) S atom being offset from a hollow site yet higher above the surface, suggesting that this S atoms does not form a S-Au chemisorption bond. A more recent SXRD investigation of the $(2\sqrt{3}\times 3)\text{rect.}$ phase of hexadecylthiolate ($n=16$) [46], however, based on a very much larger data set than that which appears to have been used in the original 1994 study, concluded that the two inequivalent S headgroup adsorption sites were the fcc and hcp hollow sites. This investigation sought to minimise the problem of the coexistence of the $(\sqrt{3}\times\sqrt{3})R30^\circ$ and $(2\sqrt{3}\times 3)\text{rect.}$ phases by concentrating the analysis on the intensity measurements of the diffraction beams that are unique to the $(2\sqrt{3}\times 3)\text{rect.}$ phase.

Perhaps as a result of the original controversy, and of the lack of further experimental information at that time, quite a number of groups conducted total energy calculations to try to determine the theoretical minimum energy structure of the Au(111)/thiol interface. These calculations mostly focussed on the simplest possible problem, namely the Au(111) $(\sqrt{3}\times\sqrt{3})R30^\circ$ -CH₃S surface phase. Clearly this involves only a single S site, and the absence of a long alkyl chain overcomes the problems of accurately treating the weak intermolecular van der Waals forces (a particular problem for DFT) in a slab calculation, or indeed of any treatment of intermolecular interactions in calculations based on small clusters. These calculations favoured a range of preferred adsorption sites: three-fold coordinated hollows [54, 55, 56, 57], two-fold coordinated bridge [58, 59, 60, 61], and an intermediate low-symmetry off-bridge site [62, 63]. These theoretical conclusions proved

to be in sharp contrast to the results of two new experimental studies of this specific adsorbate structure, one by Kondoh *et al.* using photoelectron diffraction [64], the other using NIXSW reported by Roper *et al.* [65]; both of these experiments led to clear identification of the atop site for the adsorbed S head-group atom.

This apparent incompatibility of these experimental and theoretical ‘determinations’ of the local adsorption site of methylthiolate on Au(111) (with several more recent calculations also favouring the more highly-coordinated hollow or bridging sites [66, 67]) seems to have only two possible origins. One is that the theoretical methods do not provide a reliable basis for calculating the relative energies of different binding states in this system. This possibility should not be rejected lightly; there is a well-documented example of the failure of standard DFT methods to identify correctly the preferred adsorption site for CO on Pt(111) at low coverage [68]. Several of the best groups using different DFT computer codes and different functionals have found a consistent result is a lower energy for adsorption of CO at three-fold coordinated hollows [68], yet it is fully accepted that the experimental situation shows a clear preference for atop sites. Whatever the reasons for these failures [69, 70, 71], they are a clear reminder of the fact that such theoretical calculations are not invincible. Thiulates on Au(111) *could* be a further example of this type of failure. However, an alternative explanation is that these theoretical studies simply did not test the correct structural model; as in experimental determinations of surface structure, the true minimum energy structure can only be identified in these theoretical calculations if the correct structural model is tested.

4.2 Reconstruction and Au adatoms

There is now some evidence that this possibility may hold the key to the problem, because some recent experimental and theoretical studies indicate that thiolate-induced reconstruction may also occur on the Au(111) surface. In fact, it has been clear for many years that some restructuring of this surface occurs as the thiolate SAM forms, because the clean Au(111) surface is, itself, reconstructed, and this reconstruction is lifted as the thiolate coverage increases [72]. In particular, the outermost atomic layer of clean

Au(111) adopts a uniaxially-compressed hexagonal close-packing leading to an Au-Au interatomic spacing smaller than that of the underlying bulk [73, 74, 75]. The atomic density of this layer is 4.4% larger than that of the bulk layers below, and this surface layer rumples over the substrate to give a $(23\times\sqrt{3})_{\text{rect.}}$ commensurate mesh and the characteristic ‘herring-bone’ pattern of corrugation in STM images. Loss of this reconstruction to a bulk-like surface termination must therefore lead to considerable Au atom motion with the release of this excess of Au atoms, and indeed STM images characteristically show small pits in the surface, identified as Au atom vacancy islands [72], which could, perhaps, be one consequence of incomplete redistribution Au atoms into a perfectly ordered surface. More recent results, however, show the situation is more complex than this. Until recently, it had been assumed that the ‘unreconstruction’ associated with the lifting of the herring-bone reconstruction simply led to a local (1x1) bulk-terminated surface Au layer. Recent experiments indicate that surface thiolate species are attached to Au adatoms [76, 77], rather than Au atoms in such a bulk-terminated layer, and that it is the movement of these Au-adatom-thiolate moieties that order to produce the SAM structure.

Two rather different models of these Au-adatom-thiolate moieties have emerged from different experiments. Low temperature STM imaging conducted at low coverages (only a few % of a monolayer) on the methylthiolate species [76] provides evidence for an Au-dithiolate moiety in which the Au adatom occupies a bridge site relative to the underlying Au(111) surface layer; the two S headgroup atoms are bonded to opposite sides of this adatom such that they occupy near-atop sites relative to the underlying Au surface atoms (fig 5). Notice that within this structure the thiolate S atoms actually adopt a two-fold coordinated bridging geometry, bonding both to the Au adatom and the Au surface atom directly below. A particularly interesting aspect of this study is the observation of local one-dimensional side-by-side ordering of these units, the resulting structures being similar to key ingredients of the striped phases of the longer-chain thioliates (fig. 3). Indeed, this same experimental group also observed this Au-dithiolate ordering for phenylthiolate ($n=3$) [78]. A rather different adatom-thiolate model emerged from NIXSW studies of the high coverage (0.33 ML) phases of methyl-, butyl-, hexyl- and

octyl-thiolates [77]. While the $(\sqrt{3}\times\sqrt{3})$ methylthiolate and butylthiolate ordered phases yielded NIXSW data consistent with atop site adsorption of the S headgroup on an unreconstructed Au(111) surface, the data from the longer-chain thiolates (in a mixture of $(\sqrt{3}\times\sqrt{3})$ and $(3\times 2\sqrt{3})$ rect. phases, showed the S atoms to have the same height above the Au(111) scatterer planes, but with lateral positions inconsistent with occupation of atop sites alone. Instead, the data were found to be compatible with a model in which single thiolate species are bonded atop single Au adatoms, these adatoms occupying either fcc or hcp hollow sites. Notice that NIXSW, because it measures the location of the (S) absorber atom relative to the underlying bulk, cannot distinguish between S atop a surface layer Au atom on an unreconstructed surface, and S atop an Au adatom in an fcc hollow site, because this adatom then occupies a bulk continuation site. A unifying model offered by the NIXSW data is thus that in the $(\sqrt{3}\times\sqrt{3})$ phase, all Au-thiolate moieties occupy fcc hollows, but in the $(3\times 2\sqrt{3})$ rect. these species occupy a mixture of fcc and hcp hollows.

In fact the possibility of some kind of thiolate-induced reconstruction of the Au(111) had been considered in DFT calculations prior to this experimental evidence. Specifically, Morikawa *et al.* [79] investigated the possibility of surface vacancy formation within a $(3\times 2\sqrt{3})$ rect. unit mesh of methylthiolate and found that the creation of two Au vacancies per unit mesh was energetically favoured, although the preferred adsorption site was still in an off-bridge geometry. This result, however, appeared to be sensitive to the exact mode of calculation; while favoured by a GGA (generalised gradient approximation) calculation, creating these vacancies actually cost energy in a LDA (local density approximation) calculation. At much the same date Molina and Hammer [61], explored the possibility of a thiolate-induced surface reconstruction in the $(\sqrt{3}\times\sqrt{3})$ phase of methylthiolate. Specifically, in addition to adsorption on the unreconstructed surface, these authors considered two possible reconstructions of the outermost Au atomic layer. One of these, which they refer to as the ‘honeycomb (HC) model’, has one Au surface atomic vacancy in each $(\sqrt{3}\times\sqrt{3})$ unit mesh while the second ‘inverse honeycomb (IHC) model’ has two Au surface atomic vacancies in each $(\sqrt{3}\times\sqrt{3})$ unit mesh, equivalently described as an Au(111) surface with one Au surface adatom in

each ($\sqrt{3}\times\sqrt{3}$) unit mesh. For this IHC (adatom) model they actually found the lowest energy geometry to be that with the thiolate atop the adatoms, consistent with the structure implied by the NIXSW study. However, they found the lowest energy structure to be that of bridge site adsorption on the HC model, and also found that the energy cost of creating the adatoms in the IHC model was too high to be favourable, even for the lowest-energy atop site. Notice, though, that this calculation assumed the IHC (adatom) reconstruction involved the creation of two Au surface vacancies per ($\sqrt{3}\times\sqrt{3}$) unit mesh; this ignores the intrinsic creation of adatoms by the ‘unreconstruction’ of the clean surface, and also the possibility that adatoms may be detached from surface steps at a much lower energy cost. The preference for a thiolate to adsorb in an atop geometry if there is an Au adatom on the surface was also found in calculations for ethylthiolate by Cometto *et al.* [67]; interestingly, these authors also found that the total energy of this Au-adatom-thiolate moiety was also most identical in the fcc and hcp hollow sites, and that the barrier to diffusion between these sites is very low, consistent with facile diffusion at room temperature between these sites. This result provides a rationale for the facile interchange of the ($\sqrt{3}\times\sqrt{3}$) and ($3\times 2\sqrt{3}$)rect. phases of the longer chain thiolate mentioned earlier.

DFT calculations have also been performed for the Au-adatom-dithiolate moiety proposed to occur on the basis of the low coverage STM measurements. The first such calculations were reported with the experimental measurements [76], the results showing that this surface structure is energetically favoured over the lowest energy structure on the unreconstructed surface, although in this case the calculation appears to assume the existence of an Au adatom (in the fcc hollow site) prior to the thiolate attachment. More recently, Grönbeck and Häkkinen [80] have performed calculations on both of the adatom models discussed above, and on a third adatom model in which Au adatoms occupy a mixture of fcc and hcp hollow sites while methylthiolate species bridge these adatoms. This last model, which they describe as a polymeric phase, they find to have the lowest energy; this model, however, is incompatible with both the photoelectron diffraction and NIXSW experimental results. These calculations also indicate an energetic preference for the dithiolate adatom model over the monothiolate adatom

moiety although here, too, a key issue is how one accounts for the energy cost of creating the Au adatoms. Also of relevance in this context are the results of an investigation by Mazzarello *et al.* [81] and Cossaro *et al.*[82] that combine DFT-based molecular dynamics (MD) simulations with experimental surface X-ray diffraction data for the $(\sqrt{3}\times\sqrt{3})$ -methylthiolate and $(2\sqrt{3}\times 3)$ rect.-hexythiolate phases, respectively, and photoelectron diffraction data for the methylthiolate phase. The MD results favour models with a significant degree of disorder (higher for the methylthiolate species), comprising coexistence of both the Au-adatom-dithiolate species and thiolate species bonding to bridging sites on the underlying surface, together with a significant concentration of surface Au vacancies. These models were then tested against the experimental results and found, with some modification in relative coverages, to be consistent. It is important to note, however, that the different experimental techniques used are sensitive to different aspects of the structure. In particular, SXRD is far more sensitive to the location of the strongly-scattering Au atoms (adatoms and surface vacancies) than to the much more weakly-scattering S (and C) atoms. The authors remark that the SXRD data are almost unaffected by the S atoms. By contrast, the photoelectron diffraction is mainly sensitive to the location of the S atoms.

At this point it is appropriate to summarise the main conclusions regarding the simplest system, Au(111)/methylthiolate, which has been investigated in detail only at low coverage (by STM) and in the 0.33 ML ordered $(\sqrt{3}\times\sqrt{3})$, phase as described above. There is clear experimental evidence from both photoelectron diffraction and NIXSW that the local adsorption site of the S atoms is atop surface Au atoms. DFT calculations consistently fail to find this adsorption site to be favoured on the unreconstructed surface, but two possible adatom-thiolate moieties have been proposed. Both involve S atoms that are locally atop Au atoms in the surface layer or in bulk continuation sites, and are thus potentially compatible with the original photoelectron diffraction and NIXSW results (although Mazzarello *et al.* argue that pure atop site adsorption is not compatible with some aspects of their photoelectron diffraction data [81]). DFT calculations appear to show that the Au-adatom dithiolate geometry is energetically favoured over the Au-adatom-monothiolate species [80]. On the other hand, it is worth noting that it is not

formally possible to form a ordered ($\sqrt{3}\times\sqrt{3}$) phase from the Au-adatom-dithiolate, because one such moiety per surface unit mesh would lead to a thiolate coverage of 0.67 ML, far above that which is sterically possible. It is perhaps worth adding that a significant co-occupation of bridging site thiolates on unreconstructed parts of the surface, that are present in the disordered model proposed by Mazzarello *et al.*, is incompatible with the NIXSW data, while this most recent investigation did not test the compatibility of the experimental data to the Au-adatom-monothiolate model.

Turning to the longer-chain thiolate species, perhaps the situation for the ‘lying-down’ or striped phases seems clearest, although the body of experimental data available is modest. However, there have been a small number of investigations of the local S adsorption site from such phases. Specifically, striped phases studied by photoelectron diffraction from hexylthiolate [83], and by NIXSW from butylthiolate [84], and octylthiolate [65, 85], all indicate the S headgroup atom to be in atop sites. The behaviour seen in STM at low coverage for pentylthiolate [78] strongly suggests the formation of Au-adatom-dithiolate species, and this moiety places the S atoms atop surface Au atoms, so ordering of this structural unit offers a unifying picture of these results. However, the early NIXSW investigation of decylthiolate [53], and a more recent NIXSW investigation of hexylthiolate [85] which yields similar structural parameter values, both appear to indicate co-occupation of two distinctly different S headgroup sites, exactly as found for the higher coverage standing-up phase. It seems, therefore, that even for the striped phases, not all the experimental data support a universal structural model based on the Au-adatom-dithiolate moiety.

Beyond those results already mentioned, quantitative structural information on the standing-up phases of the longer chain alkylthiolates remains sparse. There are two relatively recent SXRD studies, one of the ($\sqrt{3}\times\sqrt{3}$)R30° phase of dodecylthiolate [86], the other of the ($2\sqrt{3}\times 3$)rect. phase of hexadecylthiolate [46]. As remarked earlier, the long chain thiolates at high coverage invariably lead to a coexistence of the ($\sqrt{3}\times\sqrt{3}$)R30° and ($2\sqrt{3}\times 3$)rect. phases, but in the former study a surface preparation with minimal contributions from the ($2\sqrt{3}\times 3$)rect. phase was achieved. An interesting result of this

study was that the best fit to the data for a single high-symmetry adsorption site was found for the atop site, but a better fit could be obtained by a model based on co-occupation of atop and fcc hollow sites. Of course, the fact that the coverage corresponds to one molecule per surface unit mesh means that this more complex model probably implies incoherent domains of the two structures rather than some random mixing which leads to coherent interference between the two sites, and this was the conclusion of this study. As mentioned earlier, the investigation of the $(2\sqrt{3}\times 3)$ rect. phase of hexadecylthiolate [46] led to a best-fit model involving co-occupation (within the larger unit mesh) of molecules in fcc and hcp hollow sites. It is important to note, however, that both of these studies predate the more recently published evidence for the role of Au adatoms in the surface, so these structural models were not tested. In this context, though, it is interesting that both of these studies found evidence for very substantial relaxations within the outermost Au atom layers. As remarked above, correctly locating the much more-strongly scattering Au atoms is crucial to proper interpretation of SXRD from these surfaces, and the need to include these relaxations seems to confirm the view that Au atom movements are important. It would be interesting to know if alternative models, including Au adatoms, could provide a more consistent description of these data.

4.3 Summary – a unifying picture?

Perhaps the one thing that is clear from the foregoing information is that the detailed structure of the Au(111)/thiolate interface is *not* clear – there is no universal consensus. There are, however, some rather well-established results. For methylthiolate, the photoelectron diffraction and NIXSW clearly identify local atop site occupation as a key ingredient, but both results could also be compatible with adsorption on an unreconstructed surface or with either of the currently-proposed Au-adatom-thiolate models. There is rather strong evidence at low coverages for the Au-adatom-dithiolate model for both methylthiolate and somewhat longer-chain alkylthiolates from STM and DFT calculations, and the ordering at low coverage seen in STM strongly suggests that this local moiety may be the key ingredient in the striped-phase structures. Most (though not all) of the rather sparse amount of experimental quantitative structural information on

the striped phases supports this model. For the higher coverage $(\sqrt{3}\times\sqrt{3})R30^\circ$ and $(2\sqrt{3}\times 3)\text{rect.}$ phases the situation is less clear. It is not actually possible to construct a long-range ordered $(\sqrt{3}\times\sqrt{3})R30^\circ$ phase from the Au-adatom-dithiolate moiety because one such species per surface unit mesh leads to an unacceptably high (0.66 ML) coverage of the thiolates. For methylthiolate the only way to reconcile the experimental data with the presence of this moiety is by assuming a considerable degree of disorder is present, albeit with some residual average $(\sqrt{3}\times\sqrt{3})R30^\circ$ orderings, as seems to be implied by the interpretation of Mazzarello *et al.* [1]. For longer-chain alkylthiolates, in the presence of a significant occupation of the $(2\sqrt{3}\times 3)\text{rect.}$ phase, the NIXSW are specifically inconsistent with the Au-adatom-dithiolate moiety, but are consistent with an Au-adatom-monothiolate species. Of course, for these longer-chain thiolates, the low coverage Au-adatom-dithiolate, which has the alkyl chain essentially parallel to the surface, *must* be modified at high coverage as these chains tilt up away from the surface; under these conditions, there is, as yet, no evidence of any kind that the dithiolate remains energetically favoured. There is no considerable evidence of high levels of movement of Au surface atoms, so a transformation from a dithiolate to a monothiolate is certainly possible. Of course, the NIXSW results only implicate the role of Au adatoms indirectly. By contrast, SXRD, with its high sensitivity to the location of the strongly-scattering Au atoms, has far more potential to provide direct evidence for Au-adatom-thiolate moieties on the surface, but as yet the possible interpretation of such data from the higher coverage $(\sqrt{3}\times\sqrt{3})R30^\circ$ and $(2\sqrt{3}\times 3)\text{rect.}$ phases of the longer-chain alkylthiolates has not been undertaken. Clearly there is scope for considerable further work here.

5. Conclusions

On Cu(111) and Ag(111) many of the main features of chemisorbed alkylthiolate layers are now understood, with clear evidence for major reconstruction of the outermost metal surface layer to lower atomic-density structures being a key ingredient, and intermolecular interactions having some influence on the periodicity within these reconstructed layers. On Au(111), which has a far larger body of literature of

experimental studies in general, the detailed structure of the metal/thiol interface remains controversial. However, for this surface too there is now rather strong evidence for the role of adsorbate-induced reconstruction, probably in the form of the creation of Au-atom-thiolate moieties. The fact that it is the self-organisation of these species, and not of the thiolate on the unreconstructed surface, that controls the structural phases formed, is of key importance in understanding these SAM systems. For Au(111) there is still considerable scope for new experimental information (and reconsideration of the interpretation of some existing data) that should help to resolve the current controversies.

Acknowledgements

I am happy to acknowledge the invaluable role played by Rob Jones and his group at the University of Nottingham through our collaboration in the use of the NIXSW technique applied to many of the systems described here, and the many discussions that have ensued.

Figure Captions

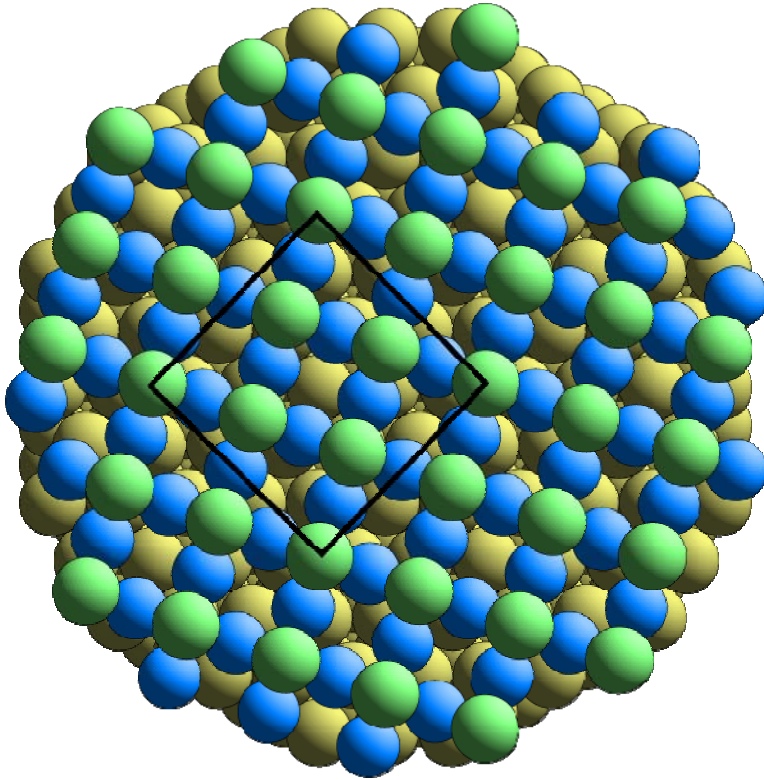


Fig. 1 Schematic plan view of the pseudo-(100) reconstruction model of the Cu(111)/methylthiolate surface phase. The thiolate species are represented by their S head-group atoms, while the outermost layer of reconstructed Cu atoms are shown with a smaller radius and different shading from those of the underlying bulk Cu atoms in order that the relative positions of the two sets of atoms can be seen. Notice, though, that the lateral registry of the reconstructed and unreconstructed layers is not known. The

probable commensurate $\begin{bmatrix} 4 & 3 \\ -1 & 3 \end{bmatrix}$ mesh is shown by the full lines.

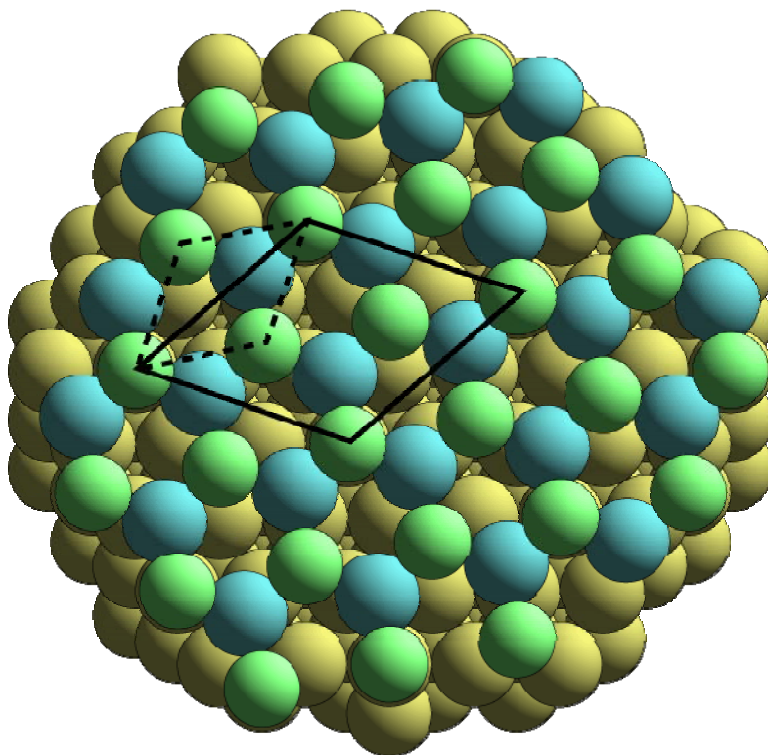


Fig. 2 Schematic plan view of the reconstruction model of the Ag(111)/methylthiolate surface phase. The thiolate species are represented by their S head-group atoms, while the outermost layer of reconstructed Ag atoms are shown with a different shading from those of the underlying bulk Ag atoms. The full lines show the commensurate $(\sqrt{7} \times \sqrt{7})R19.1^\circ$ unit mesh, while the dashed lines show the lateral sub-mesh of the S atoms alone with a local periodicity of $\sqrt{7}/3$ times that of the underlying unreconstructed Ag(111) surface.

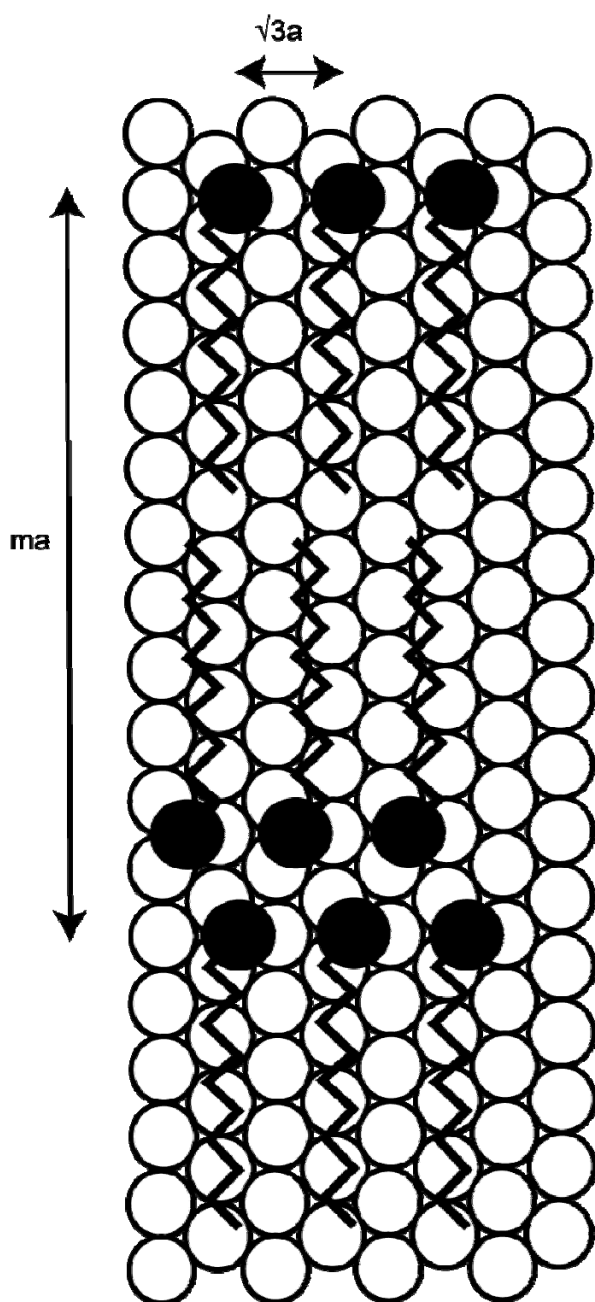


Fig. 3 Schematic diagram of a striped phase of an alkythiolate with a $(m \times \sqrt{3})$ rect. unit mesh, the alkane chain being represented by zig-zag lines. a is the Au-Au interatomic distance in the Au(111) surface. The lateral registry of the molecules and the substrate is arbitrary and does not correspond to any experimental structure determination.

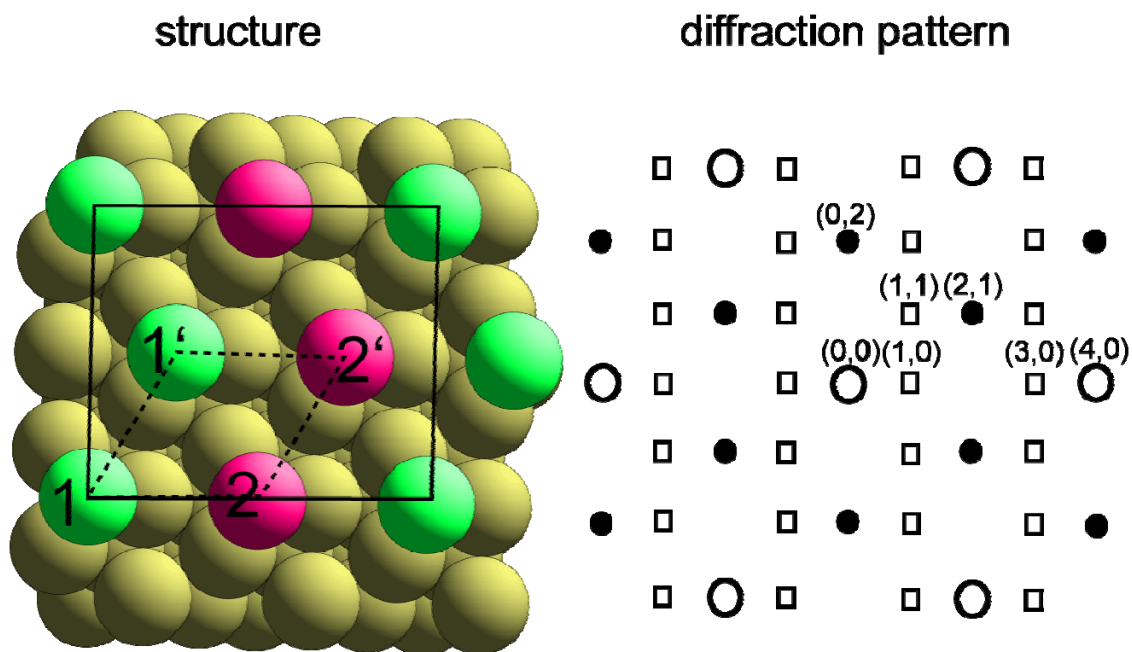


Fig. 4 Schematic plan view of a generic version of the $(3 \times 2\sqrt{3})\text{rect.}$ phase of an alkylthiolate on Au(111) and the X-ray diffraction pattern (from this single rotational domain) observed, showing the systematic ‘missing’ diffraction beams. In the diagram of the structure the thiolates are represented only by the S headgroup atoms which are (arbitrarily) shown in the fcc hollow sites, while the difference between the species labelled 1 and 1’ from those labelled 2 and 2’ are represented by a different shading. The key requirement for the structure to generate the displayed diffraction pattern is that the relative positions of the 1 and 1’ species, and of the 2 and 2’ species, are determined by coordinates $(0.25, 0.5)$ in units of the primitive translation vectors of the $(3 \times 2\sqrt{3})\text{rect.}$ unit mesh. The full lines show the $(3 \times 2\sqrt{3})\text{rect.}$ unit mesh, the dashed lines show the $(\sqrt{3} \times \sqrt{3})$ unit mesh which results if the species 1, 1’, 2 and 2’ are equivalent and in the relative positions shown in the diagram. In the diffraction pattern the large open circles show the location of the diffracted beams to be expected from the (1×1) periodicity of the substrate, while the filled circles are the positions of beams that are associated with a $(\sqrt{3} \times \sqrt{3})$ periodicity. All of these diffracted beams, together with those represented by open squares, correspond to the pattern generated by the $(3 \times 2\sqrt{3})\text{rect.}$ phase. The

labelling of the diffracted beams is in terms of the reciprocal net of the $(3 \times 2\sqrt{3})$ rect. unit mesh.

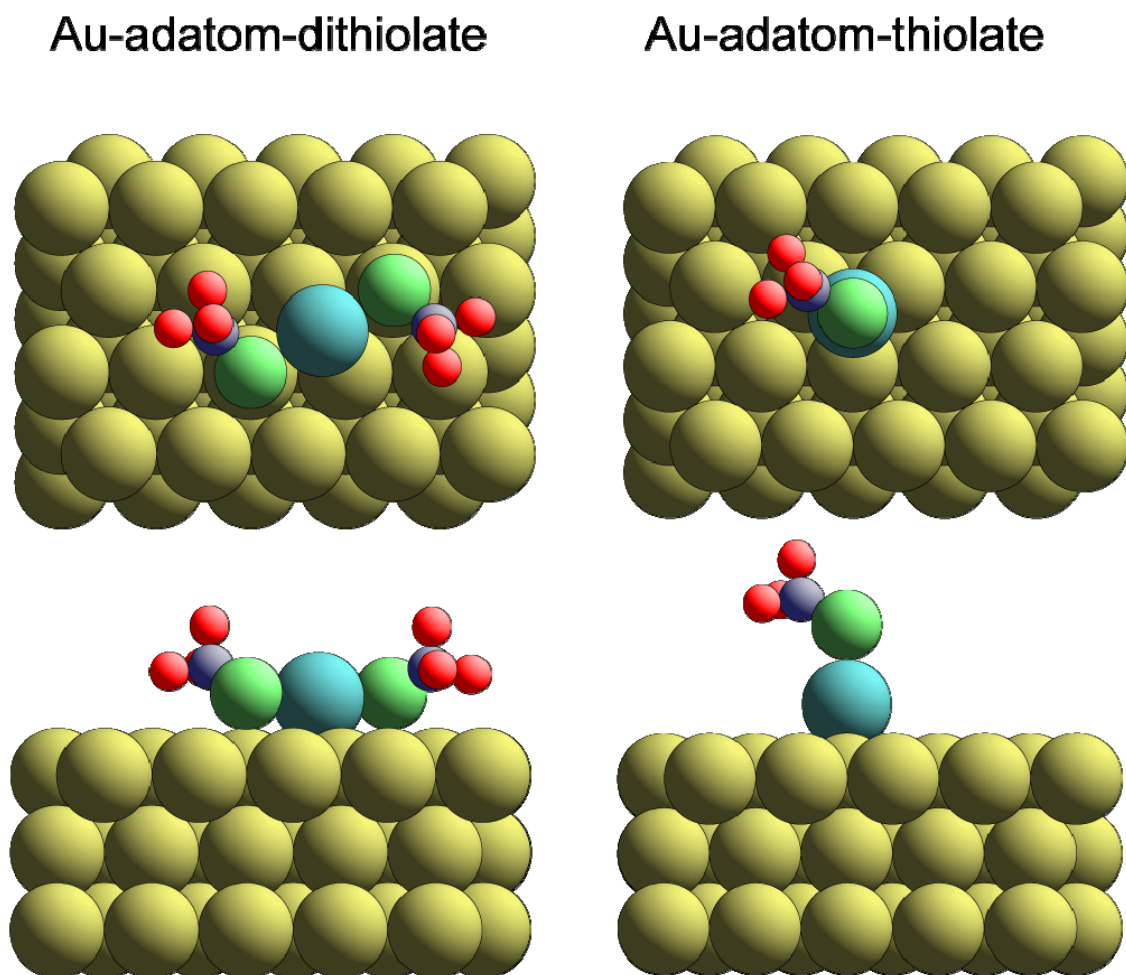


Fig. 5 Schematic diagrams, in plan and side views, of the two alternative Au-atom-thiolate moiety structures for methylthiolate that have been proposed in recent investigations, as described in the text. The Au adatoms have been shaded differently from the substrate atoms for clarity. Note that the Au-atom-thiolate model shown here has the Au adatom in the fcc hollow site; occupation of the hcp hollow site is also proposed to occur for longer alkyl chains.

References

- 1 L.H. Dubois and R.G. Nuzzo, *Annu. Rev. Phys. Chem.* 1992, **43**, 437.
- 2 A. Ulman, *Chem. Rev.* 1996, **96**, 1533.
- 3 F. Schreiber, *Prog. Surf. Sci.* 2000, **65**, 151.
- 4 C. Vericat, M. E. Vela, and R. C. Salvarezza, *Phys. Chem. Chem. Phys.* 2005, **7**, 3258.
- 5 T. Otsubo, Y. Aso, and K. Takimiya, *J. Mater. Chem.* 2002, **12**, 2565
- 6 L. M. Demers, D.S. Ginger, S.-J. Park, Z. Li, S.-W. Chung, and C.A. Mirkin. *Science* 2002, **296**, 1836.
- 7 R. A. van Delden, M.K.J. ter Wiel, M.M. Pollard, J. Vicario, N. Koumura, and B.L. Feringa *Nature* 2005, **437**, 1337.
- 8 N. P. Prince, D. L. Seymour, D. P. Woodruff, R. G. Jones, and W. Walter, *Surf. Sci.* 1989, **215**, 566.
- 9 J. Stöhr in *X-ray Absorption, Principles, Techniques, Applications of EXAFS, SEXAFS and XANES*, ed. R. Prins and D.C. Koeningsberger 1988 (Wiley, New York) 443
- 10 D. P. Woodruff, *Rep. Prog. Phys.* 1986, **49**, 683
- 11 D. P. Woodruff *Prog. Surf. Sci.* 1998, **57**, 1
- 12 D. P. Woodruff, *Rep. Prog. Phys.* 2005, **68**, 743
- 13 N. P. Prince, M. J. Ashwin, D. P. Woodruff, N. K. Singh, W. Walter, R. G. Jones, *Faraday Discuss. Chem. Soc.* 1990, **89**, 301.
- 14 S. M. Driver and D. P. Woodruff, *Surf. Sci.* 2000, **457**, 11.
- 15 J.F. van der Veen, *Surf. Sci. Rep.* 1985, **5**, 199
- 16 D. P. Woodruff, *Nucl. Instrum. Methods B* 2007, **256**, 293
- 17 G. S. Parkinson, M.A. Muñoz-Márquez, P.D. Quinn, M. Gladys, D.P. Woodruff, P. Bailey, and T.C.Q. Noakes, *Surf. Sci.* 2005, **598**, 209.
- 18 H. Rieley, G. K. Kendall, A. Chan, R. G. Jones, J. Lüdecke, D. P. Woodruff, and B. C. C. Cowie, *Surf. Sci.* 1997, **392**, 143.
- 19 S. M. Driver and D. P. Woodruff, *Langmuir*, 2000, **16**, 6693.
- 20 S.M.Driver, and D.P.Woodruff, *Surf.Sci.* 1999, **442**, 1
- 21 D. P. Woodruff, *J. Phys.: Condens. Matter* 1994, **6**, 6067.

-
- 22 M.S. Kariapper, C.J. Fisher, D.P. Woodruff, B.C.C. Cowie, and R.G. Jones, *J.Phys.:*
Condens. Matter 2000, **12**, 2153.
- 23 F. Allegretti, D.P. Woodruff, V.R. Dhanak, C. Mariani, F. Bussolotti, and S.
D'Addato, *Surf. Sci.* 2005, **598**, 253.
- 24 H. Kondoh, N. Saito, F. Matsui, T. Yokoyama, T. Ohta, and H. Kuroda, *J. Phys.*
Chem. B 2001, **105**, 12870.
- 25 F. Allegretti, F. Bussolotti, D. P. Woodruff, V. R. Dhanak, M. Beccari, V. Di Castro,
M.G. Betti, C. Mariani, *Surf. Sci.* 2008, **602**, 2453.
- 26 D.P.Woodruff, in *The Chemical Physics of Solid Surfaces*, eds. D.A.King and
D.P.Woodruff 1994 (Elsevier, Amsterdam) **7**, 465
- 27 G.J. Jackson, S.M. Driver, D.P. Woodruff, B.C.C. Cowie, and R.G. Jones, *Surf.Sci.*
2000, **453**, 183.
- 28 S.M.Driver and D.P.Woodruff, *Surf.Sci* 2001, **479**, 1.
- 29 A. L. Harris, L. Rothberg, L. H. Dubois, N. J. Levinos, L. Dhar, *Phys. Rev. Lett.* 64
(1990) 2086.
- 30 K. Schwaha, N. D. Spencer, R. M. Lambert, *Surf. Sci.* 81 (1979) 273.
- 31 R. Heinz, J. P. Rabe *Langmuir* 11 (1995) 506.
- 32 Miao Yu, S.M. Driver, D.P. Woodruff, *Langmuir* 21 (2005) 7285.
- 33 Miao Yu, D.P.Woodruff, N. Bovet, C.J. Satterley, K. Lovelock, Robert G. Jones, V.
Dhanak, *J. Phys. Chem. B* 110 (2006) 2164
- 34 G. S. Parkinson, A. Hentz, P. D. Quinn, A. J. Window, D. P. Woodruff, P. Bailey, T.
C. Q. Noakes, *Surf. Sci.* in press
- 35 D. Torres, P. Carro, R.C. Salvarezza, and F. Illas, *Phys. Rev. Lett.* 2006, **97**, 226103.
- 36 P. Fenter, P. Eisenberger, J. Li, N. Camillone III, S. Bernasek, G. Scoles, and T. A.
Ramanarayanan, K. S. Liang, *Langmuir*, 1991, **7**, 2013.
- 37 A. Dhirani, M. A. Hines, A. J. Fisher, O. Ismail, and P. Guyot-Sionnest, *Langmuir*,
1995, **11**, 2609.
- 38 Miao Yu, D.P.Woodruff, C. J. Satterley, R.G. Jones, and V. R. Dhanak, *J. Phys.*
Chem. C, 2007, **111**, 10041.
- 39 H. Rieley, G. K. Kendall, R. G. Jones, and D. P. Woodruff, *Langmuir*, 1999, **15**, 8856.

-
- 40 G.E. oirer, W.P. Fitts, and J.M. White, *Langmuir*, 2001, **17**, 1176.
- 41 e.g. E. Barrena, E. Palacios-Lidón, C. Munuera, X. Torrelles, S. Ferrer, U. Jonas, M. Salmeron, and C. Ocal, *J. Am Chem. Soc.*, 2004, **126**, 385 and references therein
- 42 B. Lüssem, L. Müller-Meskamp, S. Karthäuser, and R. Waser, *Langmuir*, 2005, **21**, 5256.
- 43 A. Riposan and G.-Y. Liu, *J. Phys. Chem. B*, 2006, **110**, 23926.
- 44 P. Fenter, P. Eisenberger, and K.S. Liang, *Phys. Rev. Lett.*, 1993, **70**, 2447.
- 45 P. Fenter, A. Eberhardt, and P. Eisenberger, *Science*, 1994, **266**, 1216.
- 46 X. Torrelles, E. Barrena, C. Munuera, J. Rius, S. Ferrer, and C. Ocal, *Langmuir*, 2004, **20**, 9396.
- 47 C. Vericat, G. Andreasen, M.E. Vela, H. Martin, and R.C. Salvarezza, *J. Chem. Phys.*, 2001, **115**, 6672.
- 48 H. Kondoh and H. Nozoye, *J. Phys. Chem. B*, 1999, **103**, 2585.
- 49 V. De Renzi, R. Di Felice, D. Marchetto, R. Blagi, U. del Pennino, and A. Selloni, *J. Phys. Chem. B*, 2004, **108**, 16.
- 50 R.G. Nuzzo, B.R. Zegarski, and L.H. Dubois, *J. Am. Chem. Soc.*, 1987, **109**, 733.
- 51 T. Ishida, S. Yamamoto, W. Mizutani, M. Motomatsu, H. Tokumoto, H. Hokari, H. Azebara, and M. Fujihira, *Langmuir*, 1997, **13**, 3261.
- 52 J. Noh and M. Hara, *Langmuir*, 2000, **16**, 2045.
- 53 P. Fenter, F. Schreiber, L. Berman, G. Scoles, P. Eisenberger, and M.J. Bedzyk, *Surf. Sci.*, 1998, **412/413**, 213.
- 54 H. Sellers, A. Ulman, Y Shnidman, and J.E. Eilers, *J. Am. Chem. Soc.*, 1993, **115**, 9389.
- 55 H. Gronbeck, A. Curioni, and W. Andreoni, *J. Am. Chem. Soc.*, 2000, **122**, 3839.
- 56 Y. Yourdshahyan, H.K. Zhang, and A.M. Rappe, *Phys. Rev. B*, 2001, **63**, 081405 .
- 57 M. Tachibana, K. Yoshizawa, A. Ogawa, H. Fujimoto, and R. Hofmann, *J. Phys. Chem. B*, 2002, **106**, 12727.
- 58 T. Hayashi, Y. Morikawa, and H. Nozoye, *J. Chem. Phys.*, 2001, **114**, 7615.
- 59 M.C. Vargas, P. Giannozzi, A. Selloni, and G. Scoles, *J. Phys. Chem. B*, 2001, **105**, 9509.

-
- 60 J. Gottschalck and B. Hammer, *J. Chem. Phys.*, 2002, **116**, 784.
- 61 M.L. Molina and B. Hammer, *Chem. Phys. Lett.*, 2002, **360**, 264.
- 62 Y. Akinaga, T. Nakajima, and K. Hirao, *J. Chem. Phys.*, 2001, **114**, 8555.
- 63 Y. Morikawa, T. Hayashi, C.C. Liew, and H. Nozoye, *Surf. Sci.*, 2002, **507-510**, 46.
- 64 H. Kondoh, M. Iwasaki, T. Shimada, K. Amemiya, T. Yokohama, T. Ohta, M. Shimomura, and K. Kono, *Phys. Rev. Lett.*, 2003, **90**, 066102-1.
- 65 M.G. Roper, M.P. Skegg, C.J. Fisher, J.J. Lee, D.P. Woodruff, and R.G. Jones, *Chem. Phys. Lett.* 2004, **389**, 87.
- 66 C. Masens, M.J. Ford, and M.B. Cortie, *Surf. Sci.*, 2005, **580**, 19.
- 67 F.P. Cometto, P. Paredes-Olivera, V.A. Macagno, and E.M. Patrito, *J. Phys. Chem. B*, 2005, **109**, 21737.
- 68 P. Feibelman, B. Hammer, J. K. Nørskov, F. Wagner, M. Scheffler, R. Stumpf, R. Watwe, and J. Dumesic, *J. Phys. Chem. B.*, 2001, **105**, 4018.
- 69 A. Gil, A. Clotet, J. M. Ricart, G. Kresse, M. Garcia-Hernández, N. Rösch, and P. Sautet, *Surf. Sci.*, 2003, **530**, 71.
- 70 G. Kresse, A. Gil, and P. Sautet, *Phys. Rev. B*, 2003, **68**, 073401.
- 71 L. Köhler and G. Kresse, *Phys. Rev. B*, 2004, **70**, 165405.
- 72 G.E. Poirier, *Chem. Rev.*, 1997, **97**, 1117.
- 73 U. Harten, A.M. Lahee, J.P. Toennies, and C. Wöll, *Phys. Rev. Lett.*, 1985, **54**, 2619.
- 74 K.G. Huang, D. Gibbs, D.M. Zehner, A.R. Sandy, and S.G.J. Mochrie, *Phys. Rev. Lett.*, 1990, **65**, 3313.
- 75 J.V. Barth, H. Brune, G. Ertl, and R.J. Behm, *Phys. Rev.* , 1990, **42**, 9307.
- 76 P. Maksymovych, D. S. Sorescu, and J. T. Yates, Jr. *Phys. Rev. Lett.*, 2006, **97**, 146103.
- 77 M. Yu, N. Bovet, C.J. Satterley, S. Bengió, K.R. J. Lovelock, P. K. Milligan, R.G. Jones, D. P. Woodruff, and V. Dhanak, *Phys. Rev. Lett.*, 2006, **97**, 166102.
- 78 P. Maksymovych and J. T. Yates, Jr., private communication; P. Maksymovych, D. S. Sorescu, and J. T. Yates, Jr., to be published.
- 79 Y. Morikawa, C.C. Liew, and H. Nozoye, *Surf. Sci.*, 2002, **514**, 389.
- 80 H. Grönbeck and H. Häkkinen, *J. Phys. Chem. B*, 2007, **111**, 3325.

-
- 81 R. Mazzarello, A. Cossaro, A. Verdini, R. Rousseau, L. Casalis, M.F. Danisman, L. Floreano, S. Scandolo, A. Morgante, and G. Scoles, *Phys. Rev. Lett.*, 2007, **98**, 016102.
- 82 A. Cossaro, R. Mazzarello, R. Rousseau, L. Casalis, A. Verdini, A. Kohlmeyer, L. Floreano, S. Scandolo, A. Morgante, M.L. Klein, and G. Scoles, *Science*, 2008, **321**, 943.
- 83 T. Shimada, H. Kondoh, I. Nakai, M. Nagasaka, R. Yokota, K. Amemiya, and T. Ohta, *Chem. Phys. Lett.*, 2005, **406**, 232.
- 84 A. Chaudhuri, D. Jackson, T.J. Leretholi, D.P. Woodruff, V. Dhanak, *to be published*
- 85 Miao Yu, PhD thesis, University of Warwick, UK, 2006.
- 86 X.Torrelles, C. Vericat, M.E. Vela, M.H. Fonticelli, M.A.D. Millone, R. Felici, T.-L. Lee, J. Zegenhagen, G. Muñoz, J.A. Martin-Gago, and R.C. Salvarezza, *J. Phys. Chem. B.*, 2006, **110**, 5586.

Contents Page textual and graphical abstract

Alkylthiolate self-assembled monolayers induce major reconstructions on Cu(111) and Ag(111), and appear to involve Au-atom-thiolate moieties on Au(111).

